Supplementary Information

Elucidating the role of diverse mineralisation paradigms on bone biomechanics - a coarse-grained molecular dynamics investigation

Mahdi Tavakol, Ted J. Vaughan

Biomedical Engineering and Biomechanics Research Centre, School of Engineering, College of Science and Engineering, University of Galway, Galway, Ireland.

1.0 Supplementary figures and table

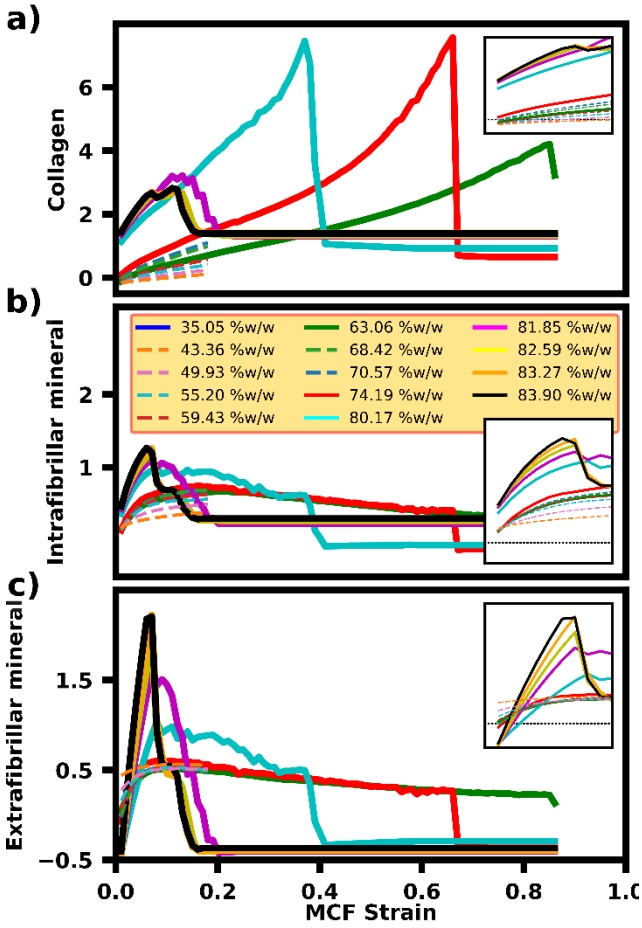

Figure S1 – The stress applied to different components of extrafibrillar mineralized MCF with 35% w/w intrafibrillar mineralization suggesting the matrix stiffness as what underlie the change in the MCF mechanical properties with extrafibrillar mineralization, while the mineralization regime determines whether the matrix or the collagen fibrils affect the UTS. Stress applied to a) collagen fibrils, b) intrafibrillar and c) extrafibrillar minerals for various overall MCF content at fixed 35% w/w intrafibrillar mineralization.

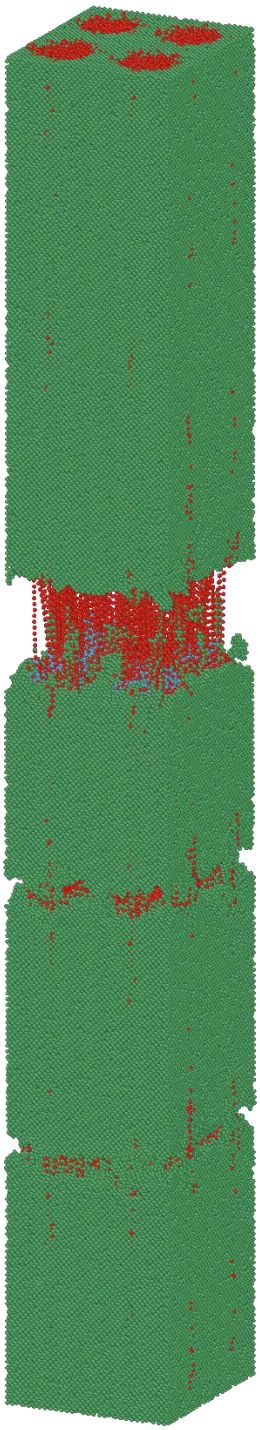

Figure S 2- The snapshot for the EFM-MCF with DoM=81.85%w/w under the external strain of 0.15 showing the crack bridging mechanism.

Table S1 – Mineralization patterns of various extrafibrillar mineralized MCF systems considered in the current study.

Simulation Set	Simulation (#)	Cutoff	Extrafibrillar Matrix Porosity (%)	$n_{collagen}$	n_{intra}	n_{extra}	iMVF (%)	iDoM (%w/w)	eMVF (%)	eDoM (%w/w)	DoM (%w/w)
1	1	9.05211	0	135780	64300	556667	13.74 ± 0.17	34.76 ± 0.33	54.59 ± 0.07	82.34 ± 0.03	83.85 ± 0.03
	2					555478					
	3					554151					
	4	9.15211			62676	556744					
	5					555555					
	6					554228					
2	7	9.05211	5	135780	64300	528999	13.74 ± 0.17	34.76 ± 0.33	53.31 ± 0.07	81.58 ± 0.03	83.22 ± 0.03
	8					527858					
	9					526335					
	10	9.15211			62676	529168					
	11					527527					
	12					526611					
3	13	9.05211	10	135780	64300	501060	13.74 ± 0.17	34.76 ± 0.33	51.96 ± 0.08	80.75 ± 0.04	82.54 ± 0.04
	14					500205					
	15					498529					
	16	9.15211			62676	501349					
	17					499676					
	18					498678					
4	19	9.05211	15	135780	64300	473499	13.74 ± 0.17	34.76 ± 0.33	50.53 ± 0.08	79.84 ± 0.04	81.80 ± 0.04
	20					472281					
	21					470607					
	22	9.15211			62676	473343					
	23					471865					
	24					470891					
5	25	9.05211	25	135780	64300	416928	13.74 ± 0.17	34.76 ± 0.33	47.40 ± 0.06	77.75 ± 0.03	80.10 ± 0.03
	26					416522					
	27					415367					
	28	9.15211			62676	416924					
	29					416514					
	30					415907					
6	31	9.05211	50	135780	64300	277786	13.74 ± 0.17	34.76 ± 0.33	37.55 ± 0.07	69.96 ± 0.04	74.10 ± 0.06
	32					277851					
	33					276901					
	34	9.15211			62676	278328					
	35					277006					
	36					277392					

7*	37	9.05211	60	135780	64300	222711	13.74 ± 0.17	34.76 ± 0.33	32.49 ± 0.05	65.11 ± 0.05	70.58 ± 0.09
	38					222287					
	39	9.15211			62676	222725					
	40					221743					
8*	41	9.05211	65	135780	64300	195233	13.74 ± 0.17	34.76 ± 0.33	29.64 ± 0.05	62.03 ± 0.06	68.42 ± 0.11
	42					194581					
	43	9.15211			62676	194890					
	44					193996					
9	45	9.05211	75	135780	64300	139174	13.74 ± 0.17	34.76 ± 0.33	23.09 ± 0.05	53.80 ± 0.05	62.92 ± 0.11
	46					138804					
	47					138500					
	48	9.15211			62676	139059					
	49					138493					
	50					138572					
10*	51	9.05211	80	135780	64300	111360	13.74 ± 0.17	34.76 ± 0.33	19.38 ± 0.01	48.25 ± 0.05	59.43 ± 0.16
	52					111230					
	53	9.15211			62676	111003					
	54					110815					
11*	55	9.05211	85	135780	64300	83351	13.74 ± 0.17	34.76 ± 0.33	15.28 ± 0.05	41.16 ± 0.11	55.20 ± 0.20
	56					83772					
	57	9.15211			62676	83451					
	58					82851					
12*	59	9.05211	90	135780	64300	55559	13.74 ± 0.17	34.76 ± 0.33	10.74 ± 0.04	31.80 ± 0.11	49.98 ± 0.24
	60					55879					
	61	9.15211			62676	55694					
	62					55190					
13*	63	9.05211	95	135780	64300	27854	13.74 ± 0.17	34.76 ± 0.33	5.66 ± 0.04	18.88 ± 0.12	43.36 ± 0.29
	64					27847					
	65	9.15211			62676	27851					
	66					27431					
14	67	9.05211	100	135780	64300	0	13.74 ± 0.17	34.76 ± 0.33	0	0	34.90 ± 0.29
	68					0					
	69	9.15211			62676	0					
	70					0					
15	71	14.4576	0	135780	6240	560684	1.59 ± 0.05	5.12 ± 0.16	58.00 ± 0.05	82.44 ± 0.03	82.60 ± 0.03
	72					559495					
	73					558168					
	74	14.3576			6624	560636					
	75					559447					
	76					558120					
16	77	14.4576	10	135780	6240	504528	1.59 ± 0.05	5.12 ± 0.16	55.44 ± 0.03	80.87 ± 0.02	81.07 ± 0.02
	78					503536					

	79	14.3576			6624	504257					
	80					503317					
17	81	14.3576	25	135780	6240	419949	1.59 ± 0.05	5.12 ± 0.16	50.89 ± 0.02	77.88 ± 0.01	78.15 ± 0.01
	82					419491					
	83	14.4576			6624	419876					
	84					419440					
18	85	14.3576	45	135780	6240	308614	1.59 ± 0.05	5.12 ± 0.16	43.20 ± 0.06	72.10 ± 0.05	72.52 ± 0.05
	86					307524					
	87	14.4576			6624	308675					
	88					307334					
19	89	14.3576	50	135780	6240	279804	1.59 ± 0.05	5.12 ± 0.16	40.84 ± 0.03	70.12 ± 0.02	70.60 ± 0.01
	90					279842					
	91	14.4576			6624	279782					
	92					279324					
20	93	14.3576	55	135780	6240	252162	1.59 ± 0.05	5.12 ± 0.16	38.34 ± 0.04	67.89 ± 0.03	68.43 ± 0.03
	94					251939					
	95	14.4576			6624	252202					
	96					251374					
21	97	14.3576	60	135780	6240	224284	1.59 ± 0.05	5.12 ± 0.16	35.60 ± 0.05	65.27 ± 0.05	65.91 ± 0.04
	98					223889					
	99	14.4576			6624	224305					
	100					223291					
22	101	14.3576	65	135780	6240	196611	1.59 ± 0.05	5.12 ± 0.16	32.61 ± 0.07	62.19 ± 0.06	62.95 ± 0.05
	102					195976					
	103	14.4576			6624	196274					
	104					195363					
23	105	14.3576	70	135780	6240	168398	1.59 ± 0.05	5.12 ± 0.16	29.31 ± 0.07	58.50 ± 0.07	59.41 ± 0.06
	106					168108					
	107	14.4576			6624	168147					
	108					167239					
24	109	14.3576	75	135780	6240	140172	1.59 ± 0.05	5.12 ± 0.16	25.67 ± 0.05	53.99 ± 0.05	55.11 ± 0.05
	110					139753					

	111	14.4576			6624	140029					
	112					139506					
25	113	-------	0	135780	0	562178	0.00 ± 0.00	0.00 ± 0.00	58.46 ± 0.05	82.48 ± 0.03	82.48 ± 0.03
	114					560989					
	115					559662					
26–No MCF	116	-------	0	0	0	556667	-------	-------	100.00 ± 0.00	100.00 ± 0.00	100.0 ± 0.00
	117					555478					
	118					554151					
27 – d=3nm	119	9.05211	15	135780	64300	544228	13.74 ± 0.18	34.76 ± 0.33	54.04 ± 0.05	82.01 ± 0.02	83.59 ± 0.03
	120					542966					
	121	9.15211			62676	543509					
	122					542791					
28 – d=4nm	123	9.05211	28	135780	64300	544108	13.74 ± 0.18	34.76 ± 0.33	54.06 ± 0.06	82.03 ± 0.01	83.59 ± 0.02
	124					543586					
	125	9.15211			62676	544469					
	126					543391					
29- d=3nm	127	9.05211	15	135780	64300	544228	13.74 ± 0.18	34.76 ± 0.33	54.04 ± 0.05	82.01 ± 0.02	83.59 ± 0.03
	128					542966					
	129	9.15211			62676	543509					
	130					542791					
30 – d=4nm	131	9.05211	15	135780	64300	642956	13.74 ± 0.18	34.76 ± 0.33	58.15 ± 0.04	84.34 ± 0.01	85.55 ± 0.02
	132					641613					
	133	9.15211			62676	642130					

	134					641416					
31 – d=5nm	135	9.05211	15	135780	64300	692544	13.74 ± 0.18	34.76 ± 0.33	59.94 ± 0.05	85.30 ± 0.01	86.37 ± 0.02
	136					691008					
	137	9.15211			62676	691725					
	138					690969					

2.0 Supplementary Results

2.1 Mechanical behaviour of MCF with various geometry and mineralisation degrees

In the main simulations of the current study, the minimum distance between MCF is equal to d=2nm. Since the MCF-MCF distance can possibly influence their interactions and also according to Hall-Petch effect [1] the size of extrafibrillar mineral nanoparticle affects its mechanical properties, here the effect of d distance on the MCF mechanical properties is studied. To this end, two different simulation sets are discussed and presented in this section. In the first simulation set designed to exclude the effect of overall mineral amount on the results, three different systems with different d distances were considered with the porosities in the extrafibrillar mineral chosen in a way to assure the fixed overall mineralisation of 83.6 %w/w. In the second simulation set with the goal of eliminating the effect of extrafibrillar matrix mechanical properties, the same extrafibrillar mineralisation degree of 85% were chosen for systems with various d values since the porosity significantly affect the matrix mechanical properties.

The uniaxial tension test results for the first simulation set suggests a significant influence of extrafibrillar matrix porosity and/or MCF-MCF distance on the MCF mechanical properties in the fixed overall mineral content (Figure S3a). Larger distance brings about smaller stress values at the strain of 5% (inset in the Figure S3a). Increasing the d distance from 3 nm to 4 nm, MCF reaches the second regime. Since with this change in fixed overall mineralisation, the porosity in the extrafibrillar matrix increases, it is deduced that extrafibrillar matrix porosity and subsequently its mechanical properties rather than extrafibrillar mineral amount determines when the change in the stress-strain response shape occurs. Since in this simulation set both the porosity and d distance was changed, in the second simulation set different d distances with same extrafibrillar matrix porosity are considered. The stress-strain plot (Figure S3b) and the stress at strain of 5% (inset in Figure S3b) remains fixed regardless of the MCF-MCF distance implying that the change observed in the previous simulation set (Figure S3b) is only owing to the extrafibrillar porosity.

The effect of MCF-MCF distance, extrafibrillar mineralisation and the overall mineral content on UTS is depicted in Figure S3b. Increasing the extrafibrillar matrix mineralisation from e=0.85 to e=1 for the fixed distance of d=2nm as obtained from the simulation the main text the, UTS increases (the blue line in Figure S3b) which is in line with the results obtained in this section for d=4 nm (the red line). A similar trend for the Young modulus is also observed (data not shown here). Increasing the d distance in fixed extrafibrillar mineralisation of e=0.85, the UTS remains fixed (the black line). However, changing both the extrafibrillar mineralisation and d at the same time to keep the mineralisation constant (the orange line), the UTS decreases. Thus, in the current study the UTS is observed to be affected by the extrafibrillar mineral porosity and its dependence on neither the MCF-MCF distance nor the mineral amount is noticed at least for the range of parameters considered here. Similarly, a very small dependence of fracture strain on MCF-MCF distance and mineral amount is observed, while a change in this parameter with extrafibrillar mineralisation is seen (Figure S3d). Larger change in the fracture strain for d=4nm (the red line in Figure S3d) than d=2nm (The blue line) is owing to a switch in the mineralisation regime. Thus, it is concluded that out of MCF-MCF distance, overall mineral content and extrafibrillar mineral porosity, the last one influences the MCF mechanical properties.

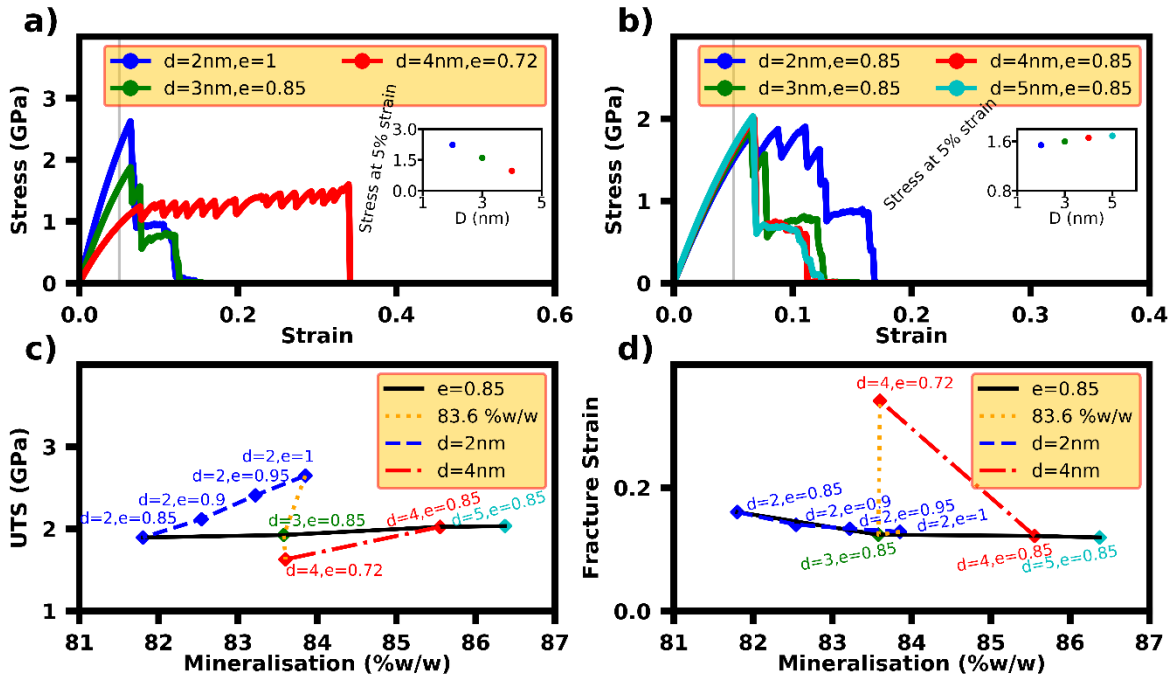

Figure S3 – The mechanical properties of MCFs with various MCF-MCF distance, extrafibrillar mineral porosity and overall mineral contents and 35% w/w intrafibrillar mineralization showing that out of the three parameters the extrafibrillar mineral porosity only influences the MCF mechanical properties. Stress-strain plots for MCFs with a) fixed overall mineral contents and various d distance and extrafibrillar mineralization and b) fixed extrafibrillar mineralization and various d distance and overall mineral contents. The summary c) the UTS and d) fracture strain for the range of MCF-MCF distance, extrafibrillar mineral porosity and overall mineral content investigated in the current study.

3.0 Supplementary discussions

3.1 Collagen and mineral residual stresses

The intrafibrillar mineralisation leads to a decrease in the collagen length which has been previously observed through both the experimental [2] and computational studies [3]. Decrease in the collagen length is due to the compressive residual stress on it which is cancelled by the same amount of residual stress in the intrafibrillar mineral in low extrafibrillar mineral amount. Specifically, in the absence of intrafibrillar minerals, the collagen beads interact with each other through bonded interactions which are in their equilibrium length and there is no residual stress at all. When the intrafibrillar minerals are added to the system as the intrafibrillar space is limited the intrafibrillar minerals are in a distance in which the mineral-mineral interaction is always attractive with the collagen beads in between not letting mineral beads distance reaching the distance with the equilibrium mineral-mineral distance. Thus, the intrafibrillar mineral is always under tensile residual stress. In low extrafibrillar mineralisation, there is a collagen shortening which decreases the residual tensile stress of the intrafibrillar mineral but still there is residual stress in this component as explained. However, when in larger extrafibrillar mineralisation, the collagen shortening is prevented which leads to a jump in the intrafibrillar mineral residual stress.

Regarding the residual stress in the extrafibrillar mineral, the potential well for the collagen-mineral is deeper than corresponding value for the mineral-mineral interactions. Thus, at low extrafibrillar mineralisation, the intrafibrillar minerals are in specific larger distances in which they exert attractive forces to each other but larger collagen-mineral interaction prevent extrafibrillar minerals move towards each other which lead to a tensile residual stress in lower extrafibrillar minerals. However, at larger extrafibrillar mineralisation, almost the whole simulation box outside collagens is filled with extrafibrillar minerals leading to a lower propensity of extrafibrillar minerals to be attracted to each other as the forces created by their neighboring

minerals cancel each other. Besides, according to the mineralisation paradigm adapted here based on the recent finding on the progress of the mineralisation from the extrafibrillar matrix to the intrafibrillar region, in higher extrafibrillar mineralistion the extrafibrillar minerals prevent the collagen shortening which translate into compressive residual stress in the extrafibrillar mineral and tensile residual stress in the collagen and intrafibrillar mineral.

3.2 Dependence of MCF-EFM stiffness on mineral amount

Simulations done in the current study alongside with results from our previous study [4] showed three different dependence of MCF stiffness on the mineral amount: (A) Larger mineralisation in systems lacking extrafibrillar mineralisation (.i.e. intrafibrillar mineralisation) brings about lower elastic modulus. (B) In fixed extrafibrillar mineralisation, increase in the mineralisation (.i.e. intrafibrillar mineralisation) has minimal influence on the elastic modulus. (C) In fixed intrafibrillar mineralisation, increase in the mineralisation (.i.e. extrafibrillar mineralisation) leads to larger Young modulus. The first two cases are discussed down below and the third one was discussed in the main text.

(A) In the absence of extrafibrillar mineralisation (the stress-strain plot with toe-heel region), the increase in the intrafibrillar mineral amount leads to larger residual strains and higher local curvatures in the MCF as shown in our previous study [4]. Besides, as mentioned in our previous study [4] and other studies on tendon [5] in the toe region the collagen straightening occurs and also a part of the residual strain is released. Thus, higher intrafibrillar mineralisation in the absence of extrafibrillar matrix leads to a larger toe-heel region and as the Young modulus is defined as the stress/strain ratio at the strain of 4%, the Young modulus in this case decreases with mineralisation. This aspect will be further investigated in a follow-up study.

(B) Regarding the case with fixed extrafibrillar mineralisation, the small deformation behavior of extrafibrillar mineralised MCF is determined either by (i) the matrix properties (highly mineralised extrafibrillar matrix) or (ii) the collagen residual strain (medium mineralised extrafibrillar matrix) (More explanation in the discussions of the main text). (i) The matrix properties are shown to be independent of the intrafibrillar mineral amount. (ii) Besides, our simulations with 5% w/w and 35% w/w intrafibrillar mineralisation, below the maximum intrafibrillar mineralisation amount of 45 %w/w in biologically relevant conditions [3], with fixed amount of extrafibrillar minerals illustrated that even though the intrafibrillar mineral slightly influenced the residual strain, the extrafibrillar mineral amount has a more significant influence. In extrafibrillar mineralised MCFs as the mineralisation starts from the extrafibrillar region to the intrafibrillar region various intrafibrillar mineral amounts have minimial effect on residual strains of systems with fixed extrafibrillar mineral. Neither (i) the extrafibrillar matrix mechanical properties nor (ii) the residual strain which affect the collagen stress-strain response are changed by the intrafibrillar mineral amount in fixed extrafibrillar mineral amount. Thus, intrafibrillar mineral amount has a moderate effect on the elastic behavior of systems with fixed extrafibrillar amount.

3.3 Comparison of simulation results with experimental findings

The stress-strain plots obtained in the current study, the stress and Young modulus values compare very well with the experimental studies in literature. For instance, a stress-strain plot with a shape similar to our highly mineralised MCF-EFMs was observed in tensile tests done by Casari et al. on hydrated micropillars extracted from ovine tibia [6]. Noticing the protruding packs of fibrils in the final fracture surface, the authors suggested the occurrence of crack-shielding mechanisms such as crack deviation and fibril bridging. Our simulation snapshots for the first mineralisation regime also implied the crack bridging by collagen fibrils in line with Casari's findings. However, in the experimental approach it was not possible to describe the series of events that led to this behaviour which was explained beforehand. Interestingly, our simulation results showed that the maximum extrafibrillar shear stress for mineralisation of 81.85 %w/w and 80.17 %w/w was 21.94±2.89 MPa and 20.28±4.03

MPa, respectively, in a good agreement with the value of 18.2 MPa estimated by Casari et al. from the results of their experiments on hydrated multiple lamellas [6]. The maximum extrafibrillar shear stress for other mineral amounts is lower than these values, though.

The shape of the stress-strain plot in the medium mineralised MCF-EFMs is similar to a typical bone stress-strain plot [7-10] up to the strain of 30%. In the post-yield region of the bone stress-strain plot, larger bone substructures affect the plastic deformation of bone. During plastic deformation, for instance debonding of osteons which belong to the higher levels in bone hierarchy (0.2 mm in size) [11] occurs in the cement line [12]. Larger bone substructures, in charge of bone plastic deformation, might eliminate the final work hardening observed in our simulations in the bone stress-strain response. The stress for the biologically relevant mineralisation amount of 60-70 %w/w for strains below the final work hardening is obtained equal to 680-800 MPa in a good agreement with the compressive strength value of 750 MPa measured on a 5000 nm micropillar made of dehydrated cortical bone [13]. These values are also similar to the stress values measured through micropillar compression tests by Ma et al. for their largest micropillar sizes of 4971 nm (900 MPa) [14]. Despite the absence of larger substructures of bone in that experimental study, still there was no work hardening prior to the final fracture in contrary to our simulation results since the final work hardening is due to the stretching of collagen molecules [15] which was not possible in microcompression experiment. Interestingly, the measured value of compressive strength for the smallest micropillar sizes of 878 nm and 640 nm (~1700 – ~2000 GPa) in the study done by Ma et al. [14] were in line with the stress values calculated in the current study for the mineralisation of 81.85 %w/w and similarly with stress fluctuations which are absent in their largest samples and similarly in our smaller mineralisation percentages including those in the biologically relevant range of 60-70% w/w. Since larger pillar sizes sample wider variations in the mineral density, there is a higher possibility that the average mineral density in the largest micropillar size be closer to the average value in the bone. However, possibility of larger or lower than biologically relevant mineralisation percents is larger in smaller pillars. That is why our simulation results for the biologically relevant mineral concentration matches the experimental results for the largest sample size and those with larger mineralisation precents explains the stress-strain plots of smaller samples. The values calculated in the current study are also in agreement with the compressive strength value of 750 MPa measured by Schwiedrzik on a 5000 nm micropillar made of dehydrated cortical bone [13]. Also, the Young modulus values between 9.61-15.69 GPa were obtained for micropillars extracted from different locations in bone by Ma et al. in another study [16] which were in a good agreement with values computed in the current study for the systems with 60-70 %w/w mineralisation.

Even though the stress values obtained in the current study are in a good agreement with micropillar compression test results [13, 14], they are larger than the results of micropillar tensile experiments done by Casari et al [6] for three possible reasons: First, as the stress values obtained by Casari et al. for the micropillar tests done in the hydrated conditions are lower than dehydrated samples [6], the lack of solvation in our system might cause larger stress values. Second, in the current study the space between lamella was ignored and the stress values were in a good agreement with the experimental results of Ma et al. in which just one single lamella was considered [13, 14]. The relative sliding in the inter lamella space which is absent in the current model might also contribute to a decrease in the bone stress value. The third reason is related to the sliding of collagen molecules. In uniaxial tension, the relative sliding of collagen molecules decreases the external loading applied to MCF [3, 17]. Even though our preliminary simulations for systems two (0.67 μm) and four times (1.34 μm) larger in length than the current system showed no length effect, there is a possibility of length effect for system sizes larger than the accessible length in the CGMD simulation in the current study. Since the length of collagen molecules is around 4.47D and neighboring collagen molecules are shifted D period in axial dimension [18], in tension two neighboring molecules can slide for up to 3.47D (4.47D-D) length before they become separated. However, the maximum possible sliding in compression is around 0.53D (5D-D) which is lowered due to the mineral incompressibility. Higher occurrence of sliding in the bone elements in tension than compression not only explains smaller stress values in tension but also implies stronger length effect for tension which is

corroborated comparing the results of these studies [6, 14]. In the micro-tensile test a decrease in the strength from 330 MPa to 140 MPa is observed with changing the sample size from 2x4x10 μm^3 (cross sectional area of 8 μm^2) to 4x8x20 μm^3 (cross sectional area of 32 μm^2) with four times the cross sectional area [6]. However, in micro-compression test to decrease the strength from 1800 MPa to 900 MPa the radius is changed from 0.32 μm (cross sectional area of 0.32 μm^2) to 2.49 μm (cross sectional area of 19.47 μm^2) [14] which is 15 times larger than the change in the size for the micro-tension test illustrating the smaller length effect in compression and importance of sliding in the tension test. Thus, stronger size effect is observed in tension than compression owing to higher importance of sliding in tension which also implies that the stress values obtained in the current study are in line with the findings in the literature.

The Young modulus for mineralisation degrees in 60-70 %w/w were calculated between 9.60±0.10 and 12.27±0.08 GPa which were in good agreement with previous experimentally measured values for macroscopic values for the elastic modulus of bovine femur [10, 19, 20] with mineralisation percent of 62±2 %w/w (Table S2) and also the microscopic elastic modulus obtained through micropillar compression tests by Ma et al. [16]. Also, the Young modulus for the systems with mineralized extrafibrillar matrix and with mineralisation percent of lower than 60 %w/w are 10-45GPa and below 10 GPa which are in agreement with experimental studies done by Karunaratne et al. on bones from healthy and impaired extrafibrillar mineralisation [21]. For MCFs with 35%w/w intrafibrillar mineralisation and total mineralisation of 74.10 %w/w the residual stress value of -73.01±2.72 MPa was calculated while the corresponding value for 5 % w/w intrafibrillar and total 70.60 %w/w mineralisation was equal to -57.60±2.64 MPa. Both the values were in agreement with the mineral residual stress values between -60 MPa and -80 MPa measured by Almer and Stock for canine fibula [22]. Two different possible reasons for having the same amount of mineral residual stress in slightly larger in-silico mineralisation than the in-vivo mineralisation of 60-70 %w/w are enumerated by the authors. First, in the 35 %w/w intrafibrillar mineralisation larger total mineralisation is needed (74.10 %w/w) than 5 %w/w intrafibrillar mineralisation (70.60 %w/w) implying that for smaller intrafibrillar mineralisation it is possible to reach the measured residual stresses in the physiologically relevant total mineralisation of 60-70 %w/w. Since the mineralisation starts from the extrafibrillar matrix towards the intrafibrillar region [23], there is a possibility for small intrafibrillar mineralisation in-vivo. Second, the presence of less mineralised elements in bone implies that amount of local mineralisation should be larger than 70 %w/w to give rise to the average mineralisation of 60-70 %w/w. Our simulations showed the occurrence of physiologically relevant mineral residual stress values in larger than 70 %w/w total mineralisation accordingly.

Table S2 – The values of the bone Young's modulus presented in the literature.

Bone type	Young modulus	Reference
Human cadaveric femurs	11.3±1.8 GPa	Wang et al. [24]
Bovine femur and tibia	20 GPa	Vashisht et al. [7]
Human femur	16.36 GPa	Zioupos and Currey [25]
Bovine haversian femur	12 GPa	Reilly and Burstein [19]
Human femur	10.1 – 13.4 GPa	Reilly and Burstein [19]
Canine fibula	24.7 GPa	Almer and Stock [22]
Human femur	16.4 GPa	Zioupos [26]
Bovine femur	11.5±3.7 GPa	Gupta et al. [10]
Osteon of human femoral midshaft	24-27 GPa	Gupta et al. [27]
Interstitial bone interface of femural midshaft	> 30 GPa	Gupta et al. [27]
Healthy mice	10-45 GPa	Karunaratne et al. [21]
Mice model with impaired extrafibrillar mineralisation	2-10 GPa	Karunaratne et al. [21]
Bovine femur	13.5 GPa	Currey [20]
Bovine femur	9.61, 15.58, 15.69 GPa	Ma et al. [16]

4.0 References

[1] S.-H. Whang, Nanostructured metals and alloys: processing, microstructure, mechanical properties and applications, Elsevier 2011.
[2] H. Ping, W. Wagermaier, N. Horbelt, E. Scoppola, C. Li, P. Werner, Z. Fu, P. Fratzl, Mineralization generates megapascal contractile stresses in collagen fibrils, Science 376(6589) (2022) 188-192.
[3] B. Depalle, Z. Qin, S.J. Shefelbine, M.J. Buehler, Large deformation mechanisms, plasticity, and failure of an individual collagen fibril with different mineral content, Journal of Bone Mineral Research 31(2) (2016) 380-390.
[4] M. Tavakol, T.J. Vaughan, A coarse-grained molecular dynamics investigation of the role of mineral arrangement on the mechanical properties of mineralized collagen fibrils, Journal of the Royal Society Interface 20(198) (2023) 20220803.
[5] P. Fratzl, K. Misof, I. Zizak, G. Rapp, H. Amenitsch, S. Bernstorff, Fibrillar Structure and Mechanical Properties of Collagen, Journal of Structural Biology 122(1) (1998) 119-122.
[6] D. Casari, T. Kochetkova, J. Michler, P. Zysset, J. Schwiedrzik, Microtensile failure mechanisms in lamellar bone: Influence of fibrillar orientation, specimen size and hydration, Acta Biomaterialia 131 (2021) 391-402.
[7] D. Vashishth, G. Gibson, J. Khoury, M. Schaffler, J. Kimura, D.P. Fyhrie, Influence of nonenzymatic glycation on biomechanical properties of cortical bone, Bone 28(2) (2001) 195-201.
[8] J.D. Currey, Role of collagen and other organics in the mechanical properties of bone, Osteoporosis International 14(Suppl 5) (2003) 29-36.
[9] H.S. Gupta, W. Wagermaier, G.A. Zickler, D. Raz-Ben Aroush, S.S. Funari, P. Roschger, H.D. Wagner, P. Fratzl, Nanoscale deformation mechanisms in bone, Nano letters 5(10) (2005) 2108-2111.
[10] H.S. Gupta, J. Seto, W. Wagermaier, P. Zaslansky, P. Boesecke, P. Fratzl, Cooperative deformation of mineral and collagen in bone at the nanoscale, Proceedings of the National Academy of Sciences 103(47) (2006) 17741-17746.
[11] R.J. Boudrieau, F. Härle, 2 - Maxillofacial bone healing, in: F.J.M. Verstraete, M.J. Lommer, B. Arzi (Eds.), Oral and Maxillofacial Surgery in Dogs and Cats (Second Edition), Elsevier, Philadelphia, 2020, pp. 6-13.e1.
[12] W.J. Landis, J.J. Librizzi, M.G. Dunn, F.H. Silver, A study of the relationship between mineral content and mechanical properties of turkey gastrocnemius tendon, Journal of Bone Mineral Research 10(6) (1995) 859-867.
[13] J. Schwiedrzik, R. Raghavan, A. Bürki, V. LeNader, U. Wolfram, J. Michler, P. Zysset, In situ micropillar compression reveals superior strength and ductility but an absence of damage in lamellar bone, Nature Materials 13(7) (2014) 740-747.
[14] Z. Ma, Z. Qiang, C. Guo, Y. Jiang, H. Zhao, C. Wen, L. Ren, Aggravated stress fluctuation and mechanical size effects of nanoscale lamellar bone pillars, NPG Asia Materials 13(1) (2021) 1-13.
[15] M.J. Buehler, S.Y. Wong, Entropic elasticity controls nanomechanics of single tropocollagen molecules, Biophysical journal 93(1) (2007) 37-43.
[16] Z. Ma, Z. Qiang, C. Guo, Y. Jiang, H. Zhao, C. Wen, L. Ren, Disparate micro-mechanical behaviors of adjacent bone lamellae through in situ SEM micropillar compression, Materials Science Engineering: A 825 (2021) 141903.
[17] B. Depalle, Z. Qin, S.J. Shefelbine, M.J. Buehler, Influence of cross-link structure, density and mechanical properties in the mesoscale deformation mechanisms of collagen fibrils, Journal of the Mechanical Behavior of Biomedical Materials 52 (2015) 1-13.
[18] J. Zhu, C.L. Hoop, D.A. Case, J. Baum, Cryptic binding sites become accessible through surface reconstruction of the type I collagen fibril, Scientific Reports 8(1) (2018) 16646.
[19] D.T. Reilly, A.H. Burstein, The elastic and ultimate properties of compact bone tissue, Journal of biomechanics 8(6) (1975) 393-405.
[20] J.D. Currey, Mechanical properties of bone tissues with greatly differing functions, Journal of biomechanics 12(4) (1979) 313-319.
[21] A. Karunaratne, C.R. Esapa, J. Hiller, A. Boyde, R. Head, J.D. Bassett, N.J. Terrill, G.R. Williams, M.A. Brown, P.I. Croucher, Significant deterioration in nanomechanical quality occurs through incomplete extrafibrillar mineralization in rachitic bone: Evidence from in-situ synchrotron X-ray scattering and backscattered electron imaging, Journal of Bone Mineral Research 27(4) (2012) 876-890.
[22] J. Almer, S.R. Stock, Micromechanical response of mineral and collagen phases in bone, Journal of structural biology 157(2) (2007) 365-370.
[23] E. Macías-Sánchez, N.V. Tarakina, D. Ivanov, S. Blouin, A.M. Berzlanovich, P. Fratzl, Spherulitic Crystal Growth Drives Mineral Deposition Patterns in Collagen-Based Materials, Advanced Functional Materials (2022) 2200504.
[24] X. Wang, R.A. Bank, J.M. TeKoppele, C.M. Agrawal, The role of collagen in determining bone mechanical properties, Journal of orthopaedic research 19(6) (2001) 1021-1026.
[25] P. Zioupos, J. Currey, Changes in the stiffness, strength, and toughness of human cortical bone with age, Bone 22(1) (1998) 57-66.
[26] P. Zioupos, J. Currey, A. Hamer, The role of collagen in the declining mechanical properties of aging human cortical bone, Journal of Biomedical Materials Research: An Official Journal of The Society for Biomaterials, The Japanese Society for Biomaterials, The Australian Society for Biomaterials 45(2) (1999) 108-116.
[27] H. Gupta, U. Stachewicz, W. Wagermaier, P. Roschger, H. Wagner, P. Fratzl, Mechanical modulation at the lamellar level in osteonal bone, Journal of materials research 21(8) (2006) 1913-1921.